LA-UR- 09-06385

Approved for public release;
distribution is unlimited.

Title:	Input Estimation From Measured Structural Response
Author(s):	Dustin Harvey, LANL, INST-OFF Elizabeth Cross, LANL, INST-OFF Ramón A. Silva, LANL, INST-OFF Chuck Farrar, LANL, INST-OFF Matt Bement, LANL, INST-OFF
Intended for:	IMAC XXVII - A CONFERENCE AND EXPOSITION ON STRUCTURAL DYNAMICS

Form 836 (7/06)

Input Estimation from Measured Structural Response

Dustin Harvey[1], Elizabeth Cross[2], Ramón A. Silva[1],
Chuck Farrar[1], Matt Bement[1]

[1)] Los Alamos National Laboratory, MS T001, Engineering Institute, Los Alamos, NM 87544

[2)] Dept of Mechanical Engineering, University of Sheffield, Sheffield, S1 3JD, UK

NOMENCLATURE

A, B, C	System state-space matrices
e	Model error
J	Cost function
J'	Perturbed cost function
ℓ	Adjoint operator
r	Test function
t	Time vector
T	Final time
u	Input guess
u'	Perturbed system states
x	System states
x'	Perturbed system outputs
y	System outputs
y_m	Measurements

ABSTRACT

This report will focus on the estimation of unmeasured dynamic inputs to a structure given a numerical model of the structure and measured response acquired at discrete locations. While the estimation of inputs has not received as much attention historically as state estimation, there are many applications where an improved understanding of the immeasurable input to a structure is vital (e.g. validating temporally varying and spatially-varying load models for large structures such as buildings and ships). In this paper, the introduction contains a brief summary of previous input estimation studies. Next, an adjoint-based optimization method is used to estimate dynamic inputs to two experimental structures. The technique is evaluated in simulation and with

experimental data both on a cantilever beam and on a three-story frame structure. The performance and limitations of the adjoint-based input estimation technique are discussed.

1. INTRODUCTION

1.1 Motivation

Knowledge of excitation to a structure can be useful for a number of different engineering applications. With a better understanding of the dynamic input to a system, the response of that system to its operational and environmental loading conditions can be more accurately determined. This information can be used to optimize design with the intent of improving system performance for failure mechanisms such as yielding, fatigue, stability or excessive deformation. However, it is not always convenient or possible to measure dynamic inputs to a system. For example, direct measurement of the input may be impractical when the excitation has a complex spatial distribution (e.g. wave loading on a ship hull) or when the structure is very large (e.g. suspension bridge subject to traffic loading). In these instances a method for estimating the inputs becomes useful. The estimation of inputs to a system constitutes an inverse problem, which has been studied for a wide variety of applications in structural dynamics (e.g. experimental modal analysis and finite element model updating).

1.2 Background

Numerous techniques based in the frequency or time domain have been used experimentally for input estimation; these include deconvolution methods, Kalman filters, dynamic programming, and gradient based methods. For the most part, research has focused on linear, time-invariant systems, involved only numerical simulations, and ignored the problem of identifying spatially-varying loads. In 1992, Carne et al. [1] developed the Sum of Weighted Averages Technique (SWAT), and applied the technique to experimentally identify the loading time-history on the nose cone of a weapon system. Later, Carne et al. [2] and Mayes [3] demonstrated the success of two methods of identifying the weighting matrix used with SWAT. In [4], an extended Kalman filter and recursive least-squares estimator were applied to a non-linear, spring-mass-damper system to reconstruct a series of various shape impulses. In simulation, the method performed admirably for a three degree-of-freedom (DOF) system. Nordstrom [5] developed a variation on the Kalman filter which was implemented in simulation on a time-variant system, and on a bridge structure with a moving input, both with excellent results.

Each of the previously mentioned techniques comes with its own set of limitations. Deconvolution methods involve an inversion of the frequency response function, which in itself is inherently unstable. The SWAT method only identifies the force applied to an object's center of mass and, therefore, cannot determine the location of inputs. Kalman filtering requires some knowledge of the expected noise in signals. Additionally, as Kalman filtering is run online, it only uses information from the previous state. In situations where the entire data history is known, a better estimate could be made at each instant combining past and future data. For this study, input estimation

will be performed using an adjoint-based optimization method. Previous applications for this technique include model predictive control and weather forecasting. The adjoint-based method developed herein has none of the above limitations but can be highly computationally and memory intensive.

1.3 Purpose

Because many structural characteristics can be determined from understanding the loading applied to a system, improved input estimations result in a better definition of the system as a whole. Previous input estimation research has shown great success in numerical simulation, but few studies have implemented the techniques on physical structures. In this work, inputs estimated by an adjoint-based optimization method are compared to those measured to evaluate its performance. This is done by implementing the method on two structures; a three-story frame structure and a cantilever beam.

1.4 Outline

This report contains an overview of the adjoint-based optimization method for input estimation in section two. A more rigorous derivation of the algorithm can be found in Appendix A. Next, the physical structures and numerical models are presented along with results of time series simulations to validate the models for this application. Section 4 presents results for estimating the input to both structures, followed by a discussion of the success of the technique along with its limitations and difficulties.

2. ADJOINT-BASED OPTIMIZATION

To begin the adjoint-based optimization, a simple cost function (based on the error between the predicted outputs and the measured outputs) is constructed; the aim is to find an input which minimizes it. To accomplish this minimization, a fairly straight forward gradient-descent process is followed. As briefly shown in Appendix A, the gradient of the cost function with respect to the input can be calculated with two simulations, regardless of the length of the input or complexity of the structure. The adjoint-based optimization method proves to have a lower computational cost when compared to a finite difference approach for estimating the gradient as only two simulations are required to generate an estimated input.

Implementation of the adjoint-based optimization method involves a few preliminary steps and a while loop to perform the iterations on the input guess. First, a model is created in state space and some guess must be made for the input. The required number of iterations is largely dependent on the accuracy of the initial input guess. For the while loop, some criterion for stopping the iterations needs to be calculated along with a threshold setting. Since the true input to the tested structures in laboratory testing can be measured directly, a metric calculated with the true input vector and the current estimate can be used as a stopping criterion. In an application where input estimation is required due to the difficulty of measuring inputs directly, a stop criterion based on the difference

between two successive input estimates could be used.

The adjoint-based optimization while loop itself contains three main steps. First, the current input estimate is used to simulate the states of the system using a numerical integration technique. Next, a test function is solved by reverse time numerical integration to calculate the gradient of the cost function with respect to the current input estimate. Finally, the gradient is used to update the input estimate using any standard gradient descent based optimization method. A line search can be used to calculate the step size for input updating. Figure 1 diagrams the adjoint-based optimization method for input estimation flowing from left to right.

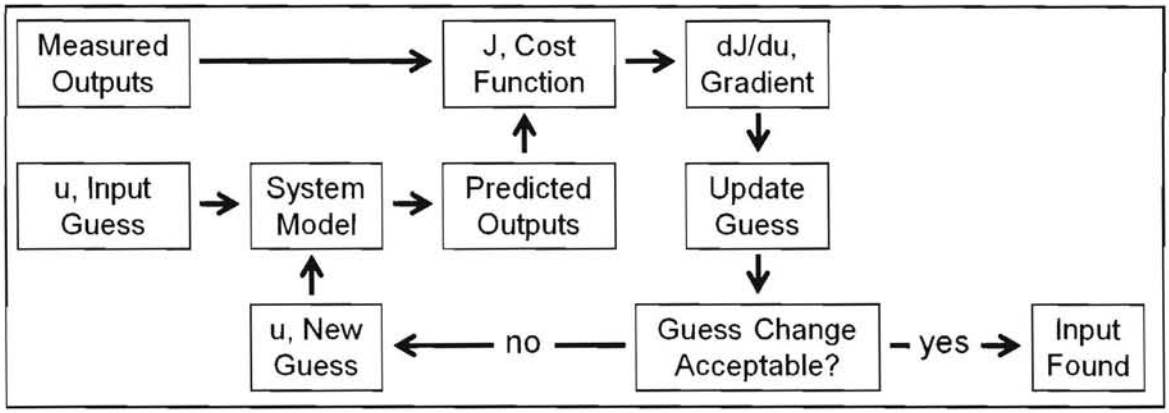

Figure 1. *Flow diagram for adjoint-based optimization input estimation*

3. STRUCTURES AND MODELING

The adjoint-based method was implemented on two structures: a three-story structure and a cantilever beam. As shown in Figure 2, the three-story structure consists of four aluminum columns (17.7 × 2.5 × 0.6 cm) which are connected to the top and bottom of each aluminum plate (30.5 × 30.5 × 2.5 cm) creating a four DOF system. Accelerometers were attached at the center line of each floor on the opposite side to the excitation source to measure the system's response. Input to the system was applied by a shaker at the base floor.

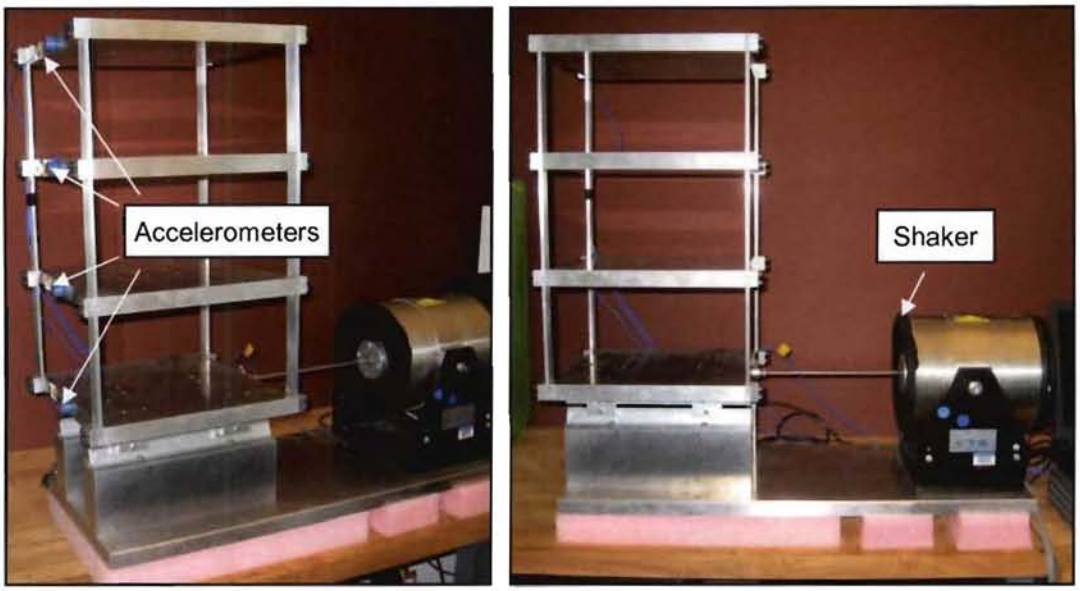

Figure 2. *Three-story structure*

To verify the accuracy and practicality of the proposed modeling approach, numerical simulations were conducted on both test structures and compared to experimental data. A four DOF lumped-mass model was constructed for the three-story structure, as shown in Figure 3. Modal Damping was added for modes 2, 3 and 4, as well as additional mass, stiffness and damping to account for the effects caused by the shaker and rails attached to the base. The response of the accelerometer was modeled with a simple low pass filter. Using a downhill simplex algorithm certain parameters were optimized, including the base's stiffness, mass and damping; the damping ratios for modes 2, 3 and 4; the accelerometer filter bandwidth; and the column stiffness. The measured and simulated accelerations due to a chirp input (25 to 75 Hz) are shown in Figure 4.

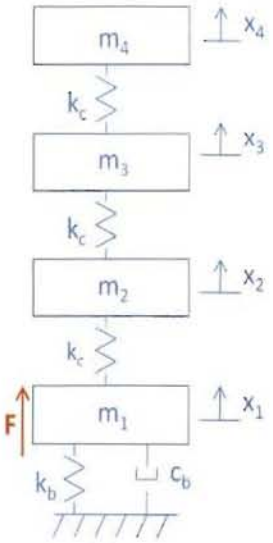

Figure 3. *Four DOF lumped mass model for three-story structure*

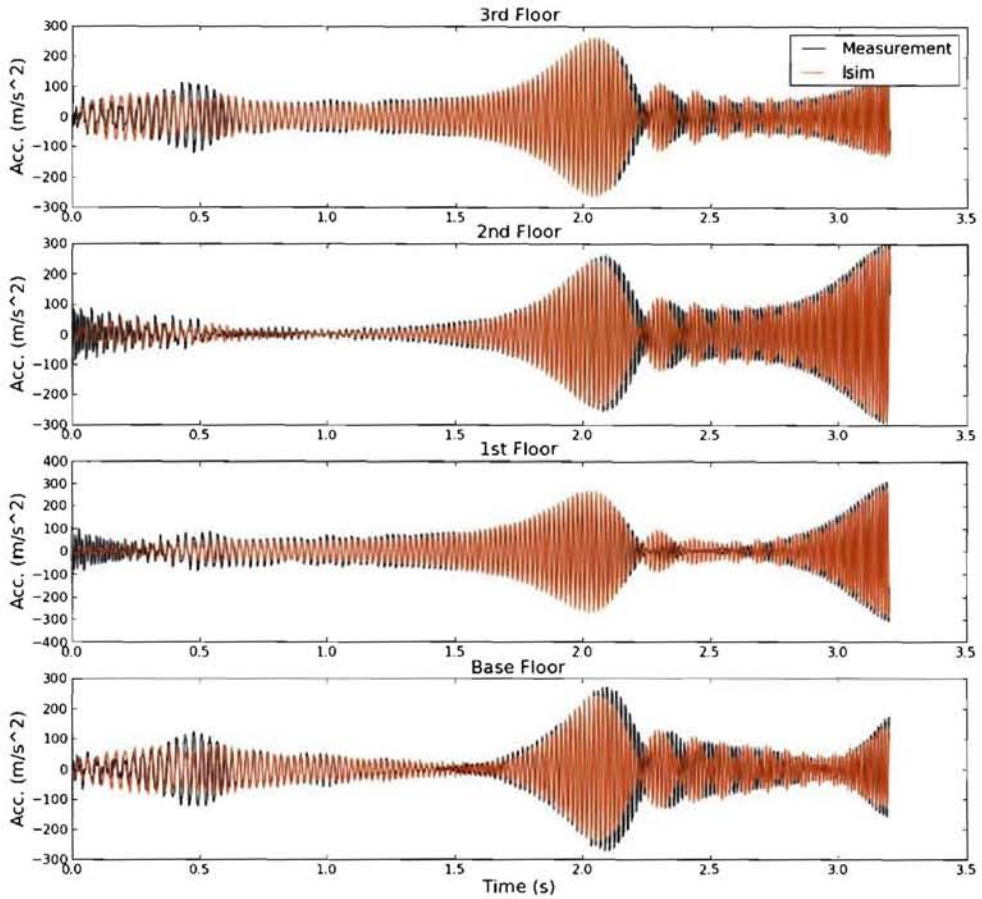

Figure 4. *Measured and simulated acceleration due to a chirp input (25 to 75 Hz)*

Figure 5 shows the cantilever beam set up; a steel L-bracket (10.2 × 10.2 × 0.95 cm) is bolted to an aluminum base (30.5 × 61 × 2.5 cm). An aluminum beam (45.7 × 5.0 × 3.2 cm) is fastened to the L-bracket by four bolts and an aluminum block (7.6 × 5 × 1.25 cm). Response of the structure was measured at the free end of the beam with an accelerometer and a CCD laser displacement sensor. A shaker was attached 5.25 cm from the fixed end of the beam to provide the input.

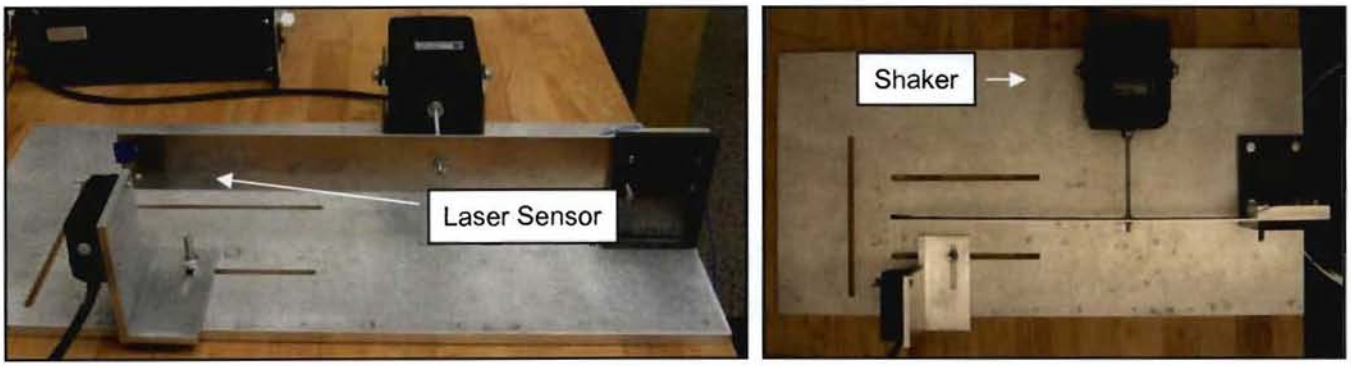

Figure 5. *Cantilever beam structure*

For the cantilever beam a finite element model was constructed using three beam elements. Additional mass, stiffness, and damping were added to the node corresponding to the input location to model the effect of the stinger and shaker. The shaker's mass, stiffness and damping were again optimized with the downhill simplex algorithm. Figure 6 shows the simulated tip displacement alongside the measurement from the laser displacement sensor for a chirp input from 15 to 25 Hz (across the first bending mode).

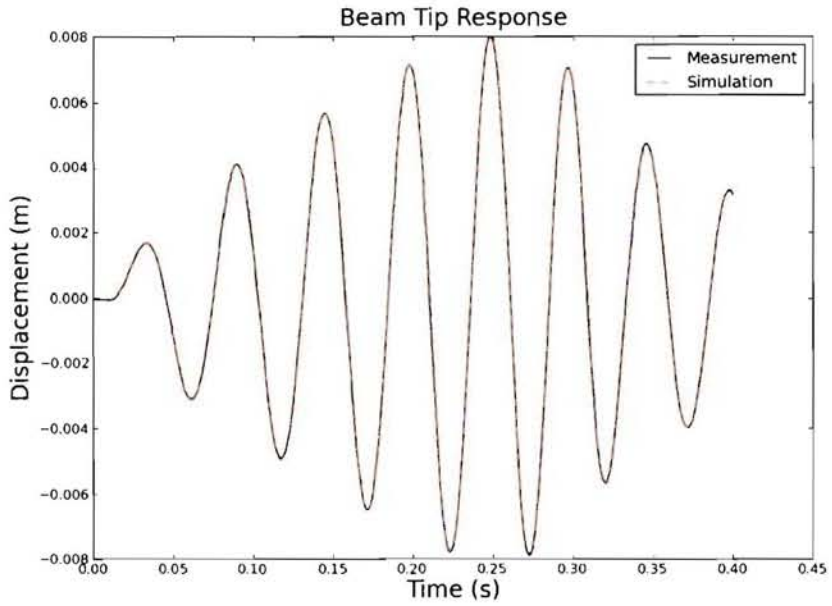

Figure 6. *Simulated and measured tip displacement*

RESULTS

Adjoint-based optimization was used to estimate various input signals applied to the cantilever beam and three-story structure. The optimization routine was first implemented using simulated response data and performed extremely well. The routine was then implemented using measured response data from the structures, which also worked successfully. Finally, for the three-story structure, the adjoint-based method was implemented using an unknown input location as well as fewer accelerometer readings. In this section estimated inputs are compared graphically to the actual inputs as measured by a force transducer.

3.1 Input Estimation for the Cantilever Beam

The adjoint-based optimization was first implemented using simulated response data. Figure 7 shows the performance of the optimization routine for a combination signal comprised of sine and triangle waves. The adjoint routine is able to recreate the input signal perfectly. This simulation comprised of 5000 data points and took 2476 iterations to converge.

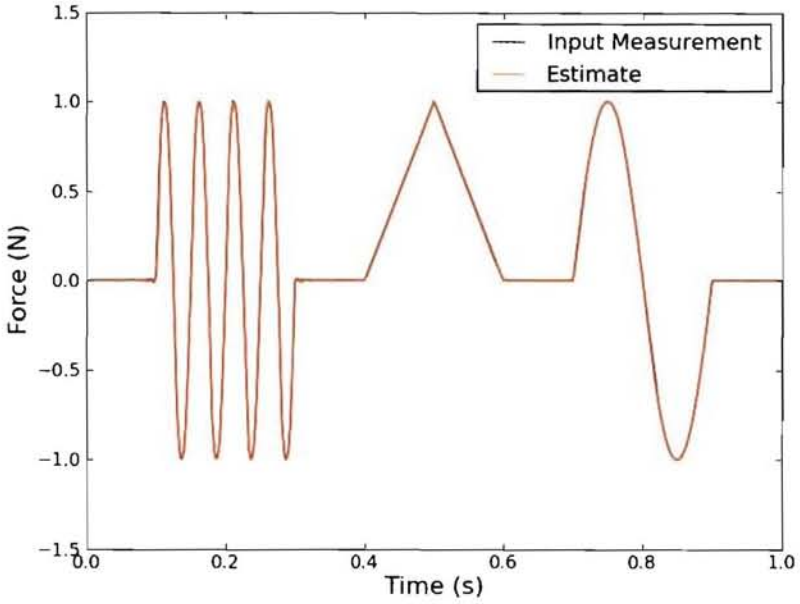

Figure 7. *Simulated input estimation of combination signal*

Next, the adjoint-based optimization method was implemented using measured response data. The cantilever beam was excited with various signals each measured with a force transducer. Figure 8 shows the time history of both the measured input (black) and estimated input (red) for a 15-25 Hz chirp input signal. The input signal was comprised of 4096 data points and took 85 iterations to converge to the specified tolerance. The adjoint-based optimization method is able to recreate the input to a reasonable degree of accuracy. The magnitude and phasing of the estimate matches the measurement well. The differences can be attributed to noise in the measurement data, unmodeled interactions between the transducer, stinger, and shaker, or the fact that the beam model cannot recreate high frequency response with only 6 degrees-of-freedom.

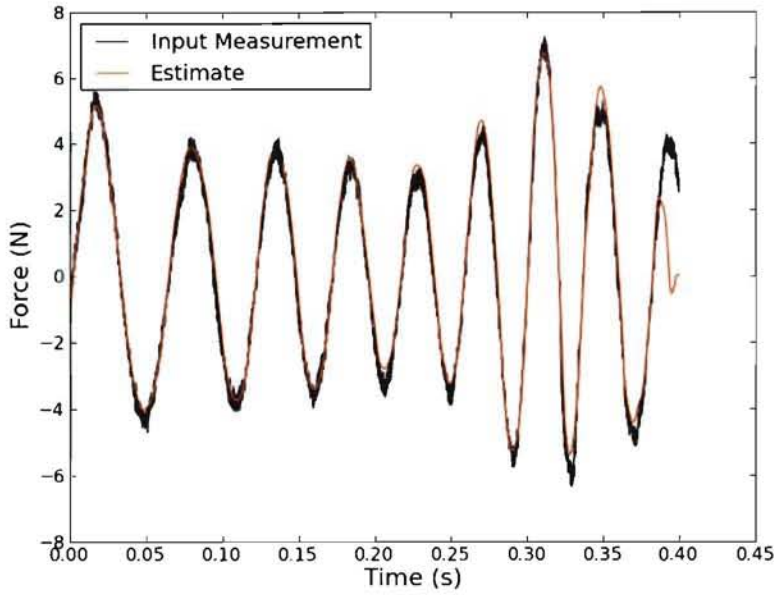

Figure 8. *Input estimation of 15-25 Hz Chirp Signal*

Figure 9 shows the performance of the adjoint method for an impulse chain excitation to the system. The impulse chain signal was composed of two square wave sections at the beginning and middle of the signal. The measurement shown from the force transducer shows the shaker's attempt to respond instantaneously to the voltage steps in the signal. The adjoint-based method was able to recreate the basic shape and magnitude of an impulse chain input. Again, some higher frequency signal components are evident in the measurements that do not appear in the estimate. The impulse chain had 4096 data points and converged in 185 iterations, more than twice as many as the chirp signal.

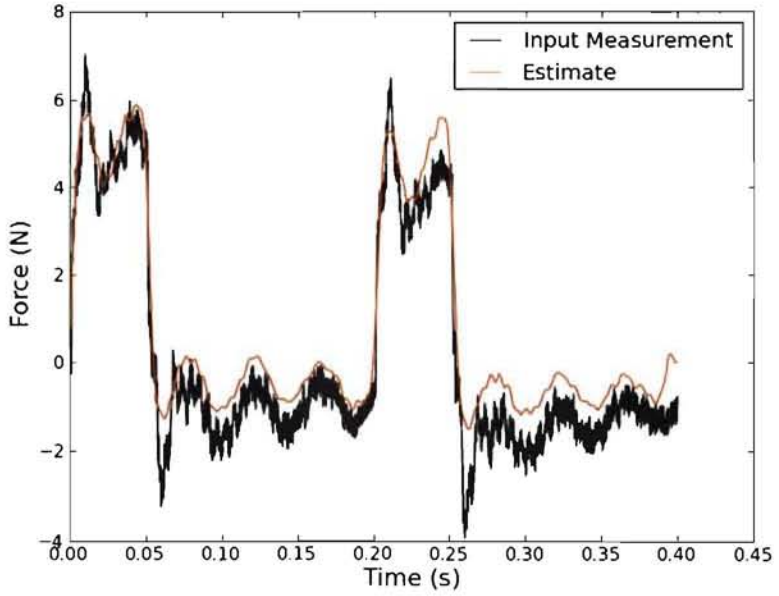

Figure 9. *Input estimation of impulse chain signal*

3.2 Input Estimation for the Three-Story Structure

As with the cantilever beam the adjoint-based optimization was first implemented on the three-story structure using simulated response data. Figure 10 shows the performance of the adjoint method for a combination signal implemented on simulated response data. This combination of sine and triangle wave signals was comprised of 5000 data points. The routine ran through 490 iterations to reach the prediction which matched the measured input perfectly.

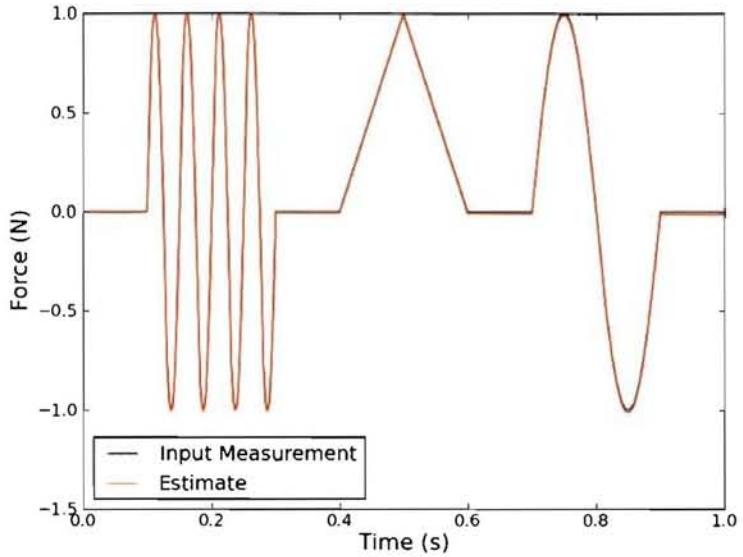

Figure 10. *Simulated input estimation of combination signal*

The adjoint-based method was next implemented using measured response to various input signals. Figures 11a, 11b, and 11c compare the time histories of the estimated signal and the measured input signal for a 45 Hz sine wave input. Enlarged sections of the datasets are provided to show the phasing of the input estimate and measurement. Figure 11c shows the force envelopes of both the measured and estimated inputs. The force envelope allows for direct comparison between the magnitude of the input estimate and measurement. The envelopes were computed using a Hilbert transform.

The sine wave input shown in Figures 11a, 11b and 11c was comprised of 16384 data points. The adjoint-based routine ran 705 iterations to produce the above estimation. Though the magnitude of the estimate is 25% too large for most of the signal, the phasing was recreated correctly.

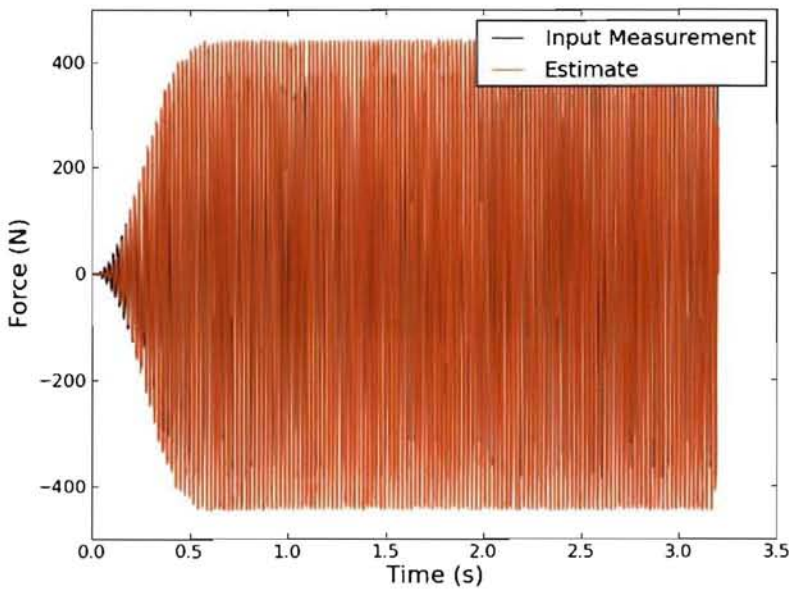

Figure 11a. *Input estimation of 45 Hz sine wave*

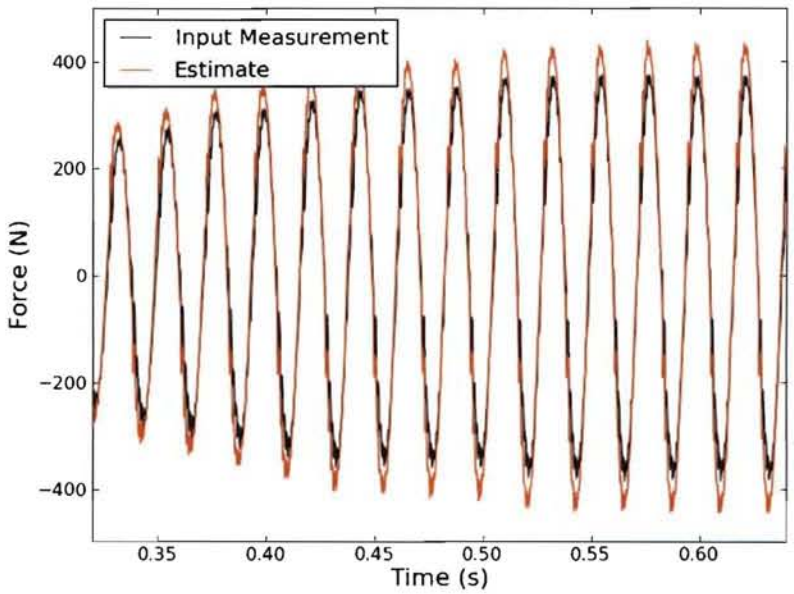

Figure 11b. *Input estimation of 45 Hz sine wave (enlarged)*

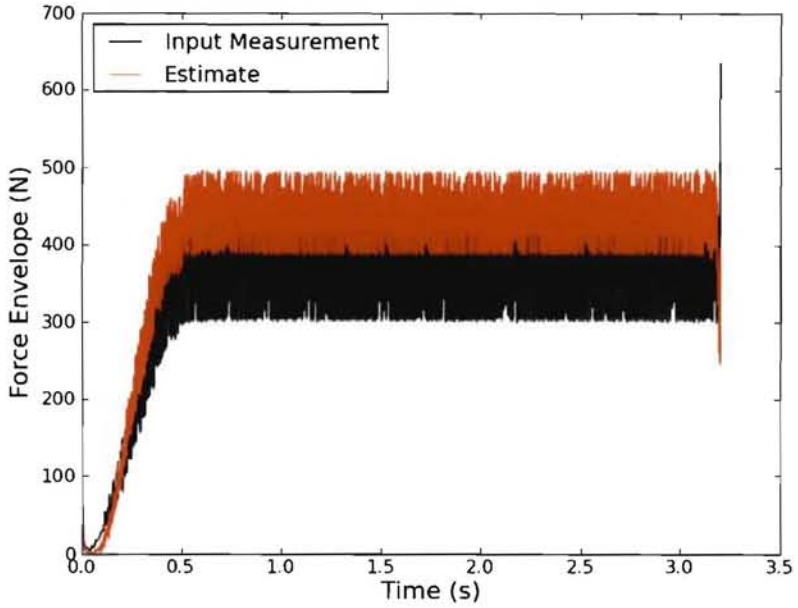

Figure 11c. *Input estimation of 45 Hz sine wave (envelope)*

Next, Figures 12a, 12b, 12c and 12d compare input estimates to experimental measurements for a 40-80Hz chirp input signal. The chirp signal was comprised of 16384 data points. The adjoint-based routine took 490 iterations to converge on this particular estimation. Figures 12a and 12b show that the estimation matches the measured input to a good degree for most of the time history. Figure 12c highlights the areas where the magnitude of the estimation does not match the measurement input as well. However, the phasing is estimated correctly throughout the signal.

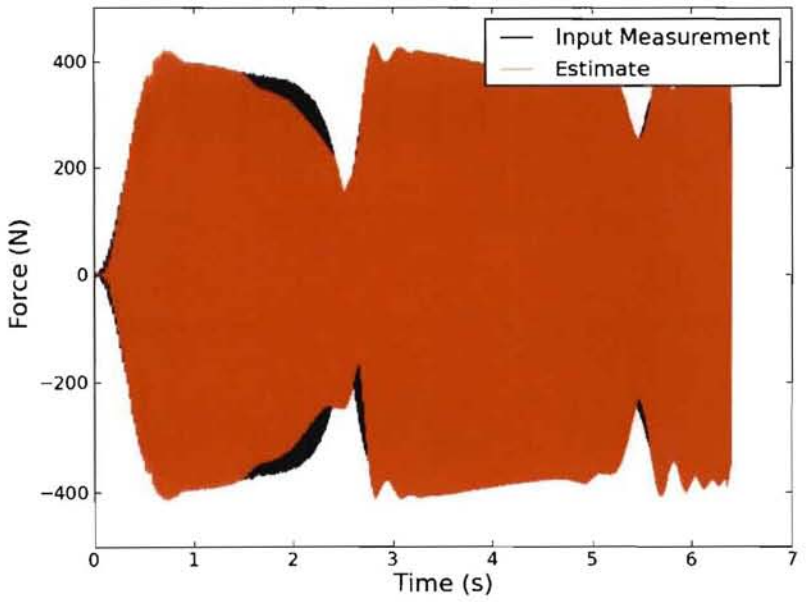

Figure 12a. *Input estimation of 40-80 Hz chirp input*

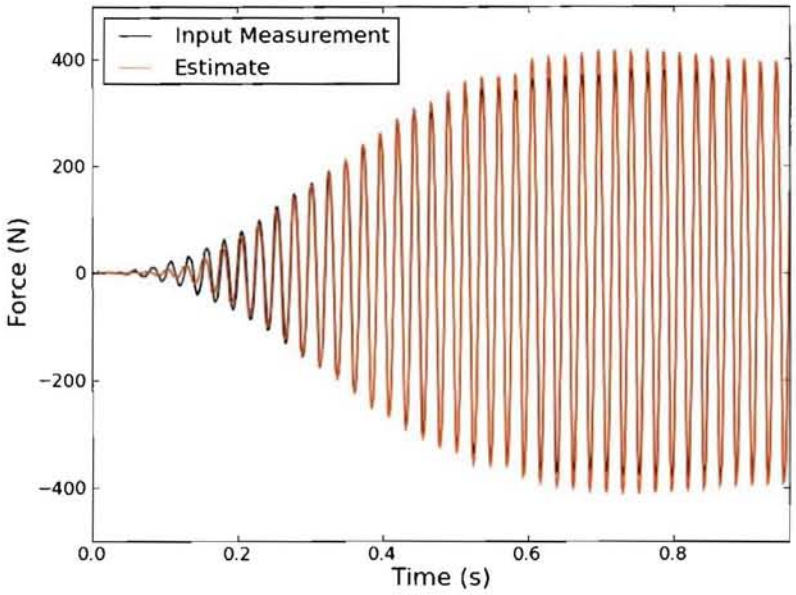

Figure 12b. *Input estimation of 40-80 Hz chirp input (enlarged)*

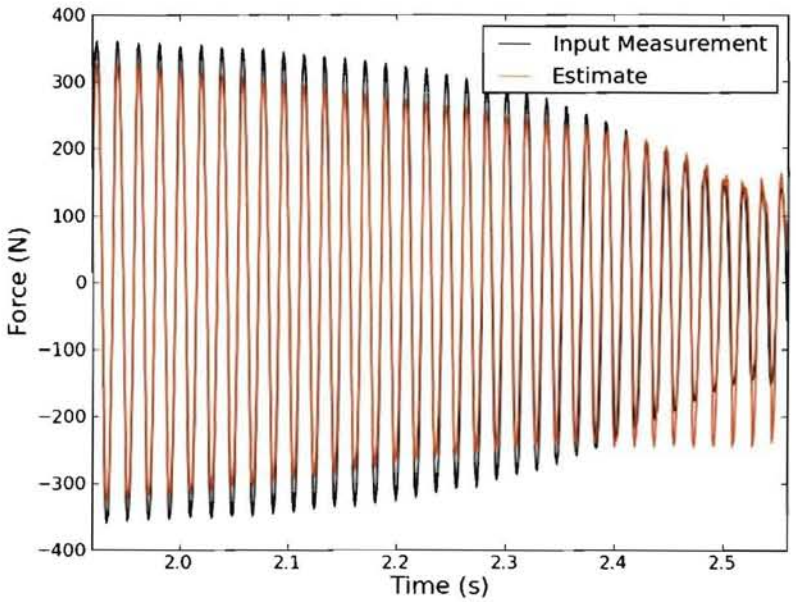

Figure 12c. *Input estimation of 40-80 Hz chirp input (enlarged)*

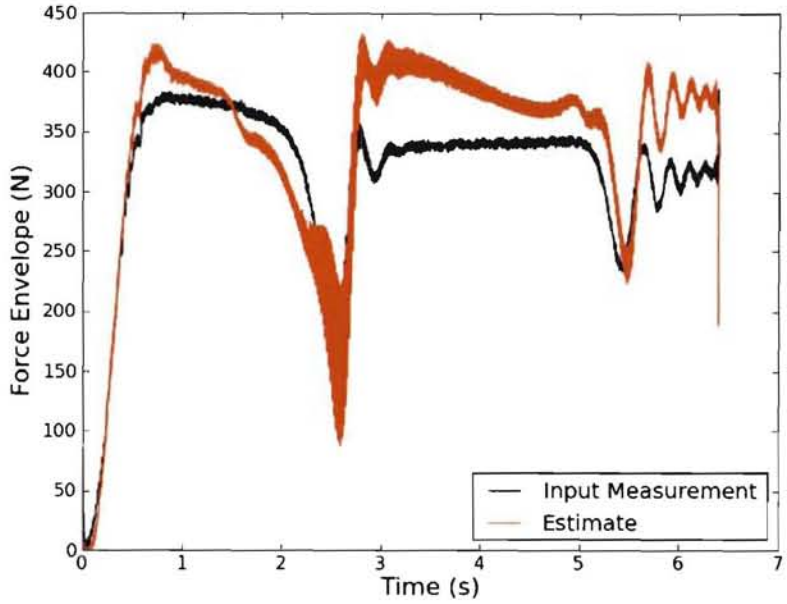

Figure 12d. *Input estimation of 40-80 Hz chirp input (envelope)*

To add more complexity input estimation was attempted with fewer accelerometers attached to the three-story structure. For this study, all accelerometers were removed except one; the system was then excited by the same 40–80Hz chirp signal used previously. Figures 13a, 13b, and 13c compare the performance of the input estimation routine with measured data for a single accelerometer placed at the base of the structure.

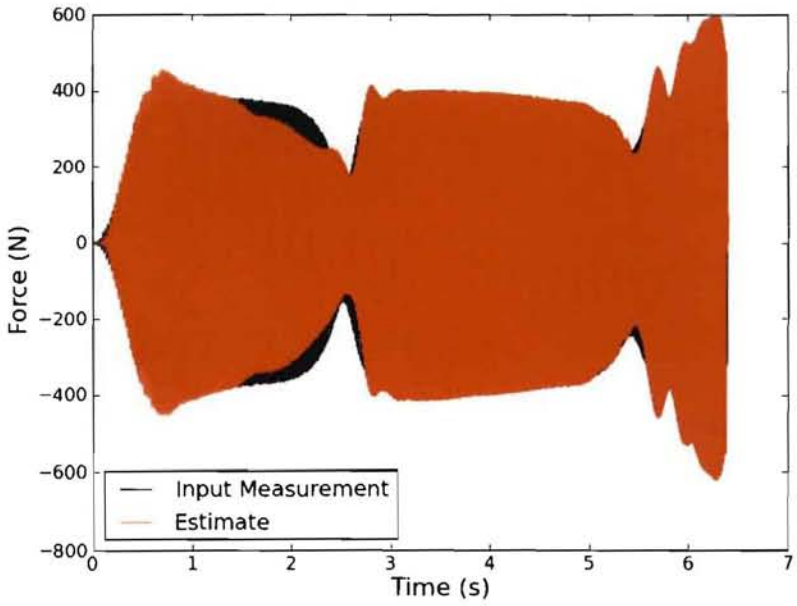

Figure 13a. *Input estimation of 40-80 Hz chirp input with base measurement only*

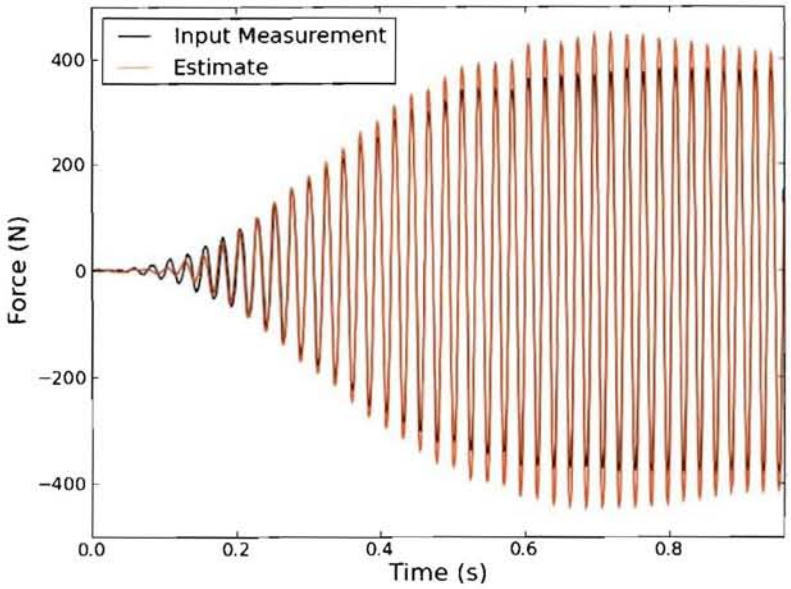

Figure 13b. *Input estimation of 40-80 Hz chirp input with base measurement only (enlarged)*

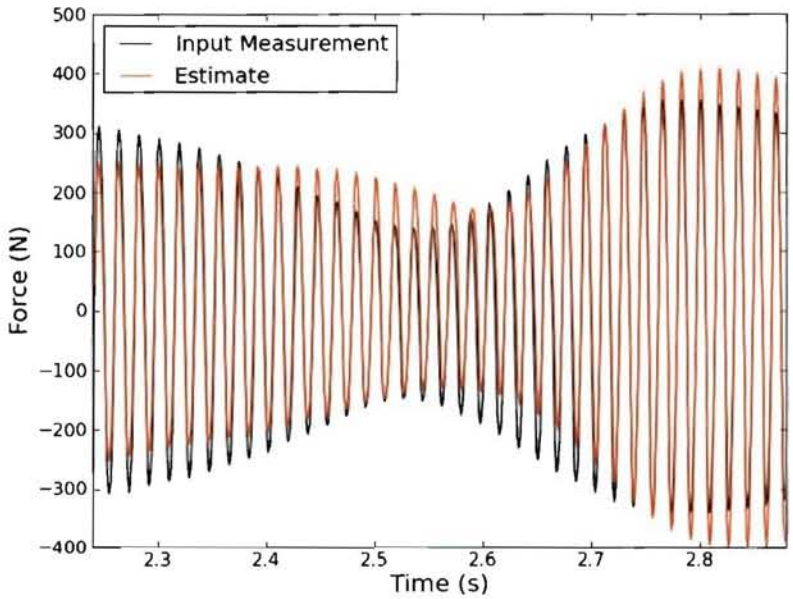

Figure 13c. *Input estimation of 40-80 Hz chirp input with base measurement only (enlarged)*

With a single accelerometer on the base floor, the adjoint routine took much longer at 7090 iterations to converge. The estimated inputs match the measured input nearly as well as with all four accelerometers. Next, an accelerometer was placed only on the third floor of the structure; the structure was then excited with the same chirp signal. Figures 14a, 14b, and 14c compare the performance of the input estimation routine with measured data for this accelerometer placement.

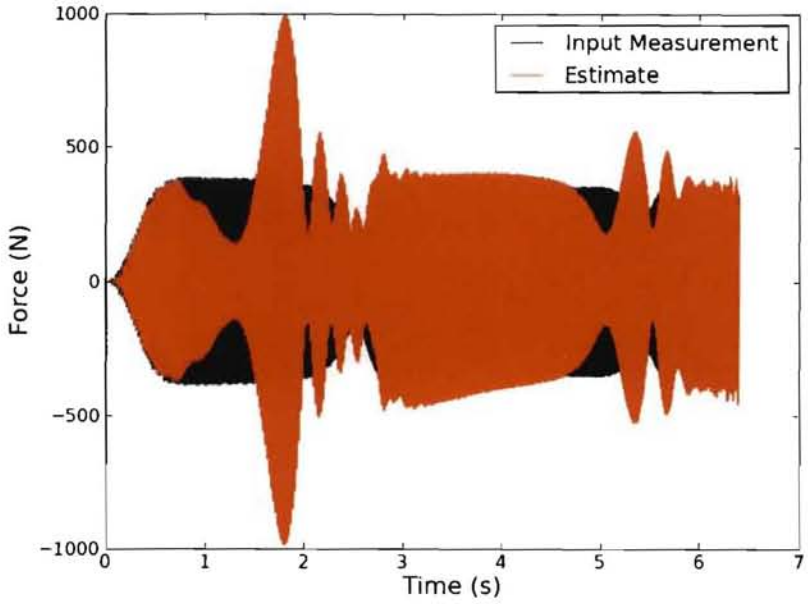

Figure 14a. *Input estimation of 40-80 Hz chirp input with third floor measurement only*

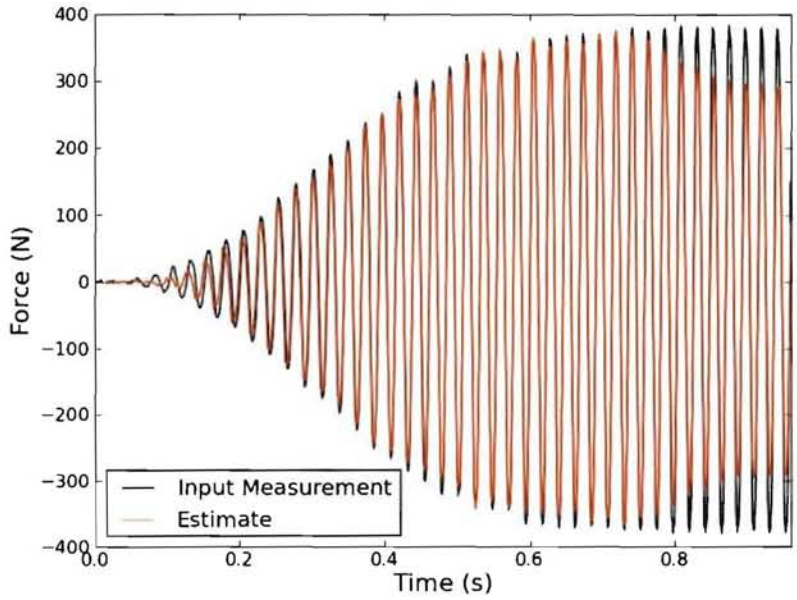

Figure 14b. *Input estimation of 40-80 Hz chirp input with third floor measurement only (enlarged)*

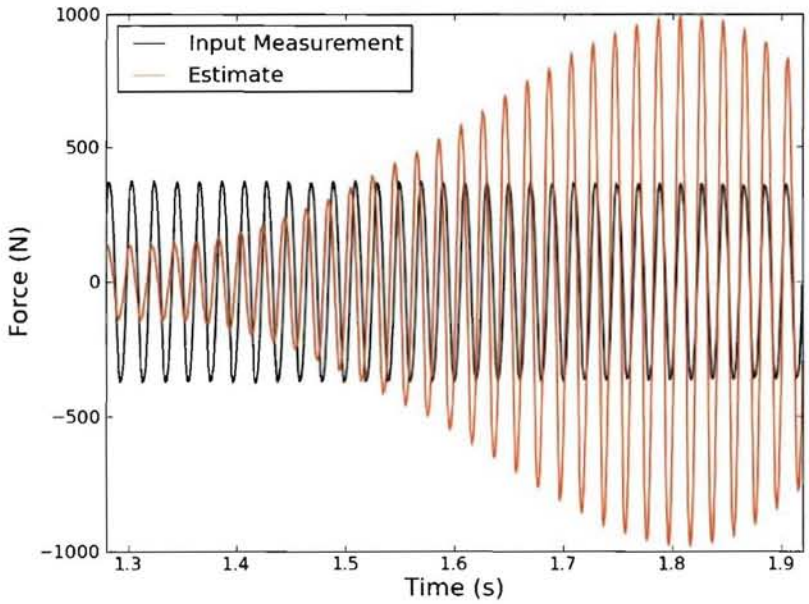

Figure 14c. *Input estimation of 40-80 Hz chirp input with third floor measurement only (enlarged)*

With the accelerometer on the top floor, the estimation converged after 16270 iterations of the adjoint-based routine. The input estimation is clearly not as accurate as when all four accelerometers or just the base accelerometer is used. Figure 14c shows problems with the estimated phase leading the measurement. From the envelopes in Figure 15, the peak magnitude of the estimate using only an accelerometer on the 3rd floor is 2.5 times larger than the true value. In comparison the trial using an accelerometer at the base estimates the magnitude to within 20% for all but the end of the signal.

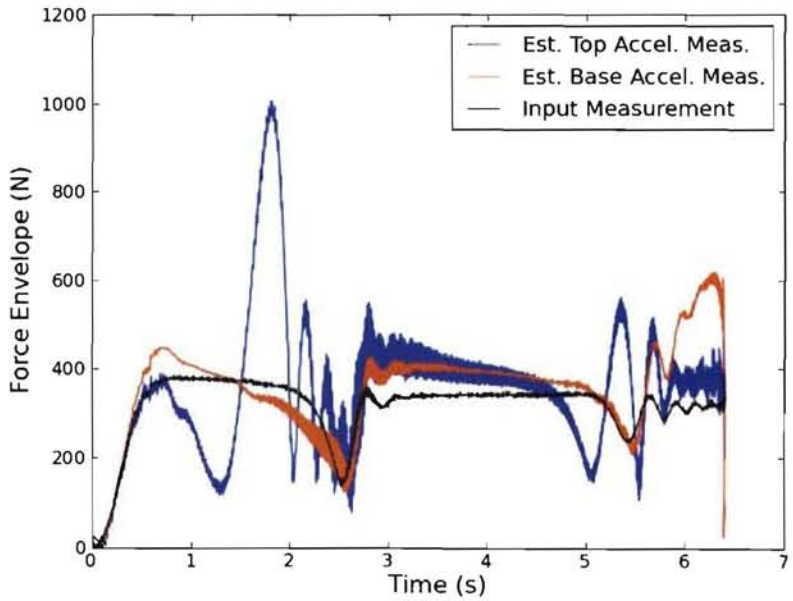

Figure 15. *Input estimation of 40-80 Hz chirp input with single accelerometer measurements (envelope)*

4. CONCLUSION

This preliminary study on implementing adjoint-based optimization techniques for use in estimating inputs to dynamic structures produced promising results. In simulation, the method is able to recreate any continuous input to any model, although for some systems many iterations of the optimization may be needed to reach a perfect estimate. For the cantilever beam structure, the adjoint-based optimization performed as well as can be expected considering the simplistic model used with only 6 degrees-of-freedom. Likewise, input estimation for the three-story structure worked well when accelerometers were placed on every floor. With limited sets of measurements, the estimate was not able to accurately reconstruct the magnitude of the input though the phasing still matched the measurement. With an improved model (particularly for energy dissipation on the three story structure), the adjoint-based optimization method would be expected to perform even better than the results shown here. The routine may also be expected to perform better for fewer response measurements if the gradient descent was changed to a global minimization technique.

REFERENCES

[1] Carne T G, Bateman V I and Mayes R L. Force reconstruction using a sum of weighted accelerations technique. 1992. Sandia National Laboratories; pp.291-298.

[2] Carne T G, Mayes R L and Bateman V I. Force reconstruction using a sum of weighted accelerations technique- max-flat procedure. 1994. Sandia National Laboratories. pp. 1053-1062.

[3] Mayes Randall L, Measurements of lateral launch loads on re-entry vehicles using SWAT. 1994. Sandia National Laboratories, Experimental Structural Dynamics Department. pp. 1063-1068.

[4] Ma C-K, Ho C-C, An inverse method for the estimation of input forces acting on non-linear structural systems. 2004. *Journal of Sound and Vibration* .pp. 953-971

[5] Nodstrom, L J L, A dynamic programming algorithm for input estimation on linear time-variant systems. 2006. *Computer Methods in Applied Mechanics and Engineering.* pp. 6407-6427

APPENDIX A

Mathematically, the details of the adjoint-optimization approach are as follows. The non-linear finite element model can be represented as

$$\dot{x} = f(x,u,t) \tag{1}$$

where *x* is the vector of system states (usually positions and velocities of all the nodes in the mesh of the structure), *u* is a vector of inputs at nodes on the structure and *t* is time. The measured outputs, *y*, can generally be represented as

$$y = Cx$$

where, *C* is some matrix. Stated another way, the outputs are some linear combination of the states of the system. The model's error is then defined to be

$$e = y - y_m$$

The goal of the optimization is to select *u* such that *e* is minimized. Or, more precisely, we want to minimize the cost function

$$J = \frac{1}{2}\int_0^T e^T e\, dt \tag{2}$$

Since $e = Cx - y_m$, after some manipulation, this cost function can be rewritten as

$$J = \int_0^T x^T Qx - 2{y_m}^T Cx + {y_m}^T y_m dt$$

where $Q=C^TC$. If the input *u* is perturbed by u', the perturbed state trajectory is given by the tangent linear equation

$$\dot{x}' = A(t)x' + B(t)u' \quad \text{or} \quad \ell x' = Bu' \tag{3}$$

where $\ell = \frac{d}{dt} - A(t)$ and *A(t)* and *B(t)* are obtained by linearizing Equation 1 about *x* and *u*. The resulting perturbation to *J* is given by

$$J' = \int_0^T x^T Qx' - {y_m}^T Cx' dt = \int_0^T \left(x^T Q - {y_m}^T C\right)x' dt \tag{4}$$

The goal of what follows is simply to re-express *J'* as a functional linear in *u'*. To that end, we integrate Equation 3 against a test function, *r*.

$$\int_0^T r^T \ell x' dt = \int_0^T r^T \left(\dot{x}' - A(t)x\right)dt$$

Using integration by parts, we can rewrite the above equation as

$$\int_0^T r^T \ell x' dt = \int_0^T (\ell^* r)^T x' dt + r^T x'\Big|_{t=0}^{t=T}$$

where $\ell^* = -\frac{d}{dt} - A(t)^T$. This is true for any test function, *r*. If we select *r* such that

$$\begin{aligned} \ell^* r &= Qx - C^T y_m \\ r(T) &= 0 \end{aligned} \tag{5}$$

where T is the final time, then Equation 4 can be rewritten as

$$J' = \int_0^T \left(x^T Q - {y_m}^T C\right) x' dt = \int_0^T \left(\ell^* r\right)^T x' dt = \int_0^T r^T \ell x' dt = \int_0^T r^T B u' dt$$

Equation 5 is referred to as the adjoint equation. Thus, we have expressed *J'* as a functional linear in *u'*. The gradient of which with respect to *u* is then simply

$$\frac{DJ}{Du} = r^T B$$

Therefore, givens some initial guess at *u*, Equation 1 is solved for *x*. This *x* is then used in conjunction with the measured data, y_m, to solve Equation 5 in reverse-time since *r(T)* is known. From *r*, the gradient of the cost function with respect to the input may be calculated, and used to update *u* (using any number of standard gradient descent based optimization techniques). Note that solving Equation 5 requires what is known as an adjoint version of the simulation code, which can calculate the linearized *A(t)* and *B(t)*, as functions of *x* and *u*. This step allows for non-linear models to be used with the technique.